



Edgar, K. M., Wilson, P. A., Sexton, P. F., Gibbs, S. J., Roberts, A. P., & Norris, R. D. (2010). New biostratigraphic, magnetostratigraphic and isotopic insights into the Middle Eocene Climatic Optimum in low latitudes. *Palaeogeography, Palaeoclimatology, Palaeoecology*, 297(3-4), 670-682. 10.1016/j.palaeo.2010.09.016

Link to published version (if available):  
[10.1016/j.palaeo.2010.09.016](https://doi.org/10.1016/j.palaeo.2010.09.016)

[Link to publication record in Explore Bristol Research](#)  
PDF-document

## University of Bristol - Explore Bristol Research

### General rights

This document is made available in accordance with publisher policies. Please cite only the published version using the reference above. Full terms of use are available:  
<http://www.bristol.ac.uk/pure/about/ebr-terms.html>

### Take down policy

Explore Bristol Research is a digital archive and the intention is that deposited content should not be removed. However, if you believe that this version of the work breaches copyright law please contact [open-access@bristol.ac.uk](mailto:open-access@bristol.ac.uk) and include the following information in your message:

- Your contact details
- Bibliographic details for the item, including a URL
- An outline of the nature of the complaint

On receipt of your message the Open Access Team will immediately investigate your claim, make an initial judgement of the validity of the claim and, where appropriate, withdraw the item in question from public view.

1 New biostratigraphic, magnetostratigraphic and isotopic insights into the Middle  
2 Eocene Climatic Optimum in low latitudes

3

4 K.M. Edgar<sup>a\*</sup>, P.A. Wilson<sup>a</sup>, P.F. Sexton<sup>a, b, c</sup>, S.J. Gibbs<sup>a</sup>, A.P. Roberts<sup>a, d</sup> and R.D.  
5 Norris<sup>b</sup>

6

7 <sup>a</sup> School of Ocean and Earth Science, National Oceanography Centre, Southampton,  
8 SO14 3ZH, UK.

9 <sup>b</sup> Scripps Institution of Oceanography, University of California, San Diego, La Jolla,  
10 CA 92093, USA.

11 <sup>c</sup> now at: School of Earth and Ocean Sciences, Cardiff University, Cardiff CF10 3YE,  
12 UK.

13 <sup>d</sup> now at: Research School of Earth Science, The Australian National University,  
14 Canberra ACT 0200, Australia.

15

16 \*Corresponding author. Tel.: +44-2380-596245; Fax; +44-2380-593052

17 E-mail address: [kme@noc.soton.ac.uk](mailto:kme@noc.soton.ac.uk)

18

### 19 ***Abstract***

20 The Middle Eocene Climatic Optimum (MECO) was a warming event that interrupted  
21 the long-term Eocene cooling trend. While this event is well documented at high  
22 southern and mid-latitudes, it is poorly known from low latitudes and its timing and  
23 duration are not well constrained because of problems of hiatus, microfossil  
24 preservation and weak magnetic polarity in key sedimentary sections. Here, we report  
25 the results of a study designed to improve the bio-, magneto- and chemostratigraphy

26 of the MECO interval using high-resolution records from two low-latitude sections in  
27 the Atlantic Ocean, Ocean Drilling Program (ODP) Sites 1051 and 1260. We present  
28 the first detailed benthic foraminiferal stable isotope records of the MECO from the  
29 low latitudes as well as biostratigraphic counts of *Orbulinoides beckmanni* and new  
30 magnetostratigraphic results. Our data demonstrate a ~750 kyr-long duration for the  
31 MECO characterized by increasing  $\delta^{13}\text{C}$  and decreasing  $\delta^{18}\text{O}$ , with minimum  $\delta^{18}\text{O}$   
32 values lasting ~40 kyrs at 40.1 Ma coincident with a short-lived negative  $\delta^{13}\text{C}$   
33 excursion. Thereafter,  $\delta^{18}\text{O}$  and  $\delta^{13}\text{C}$  values recover rapidly. The shift to minimum  
34  $\delta^{18}\text{O}$  values at 40.1 Ma is coincident with a marked increase in the abundance of the  
35 planktonic foraminifera *O. beckmanni*, consistent with its inferred warm-water  
36 preference. *O. beckmanni* is an important Eocene biostratigraphic marker, defining  
37 planktonic foraminiferal Zone E12 with its lowest and highest occurrences (LO and  
38 HOs). Our new records reveal that the LO of *O. beckmanni* is distinctly diachronous,  
39 appearing ~500 kyr earlier in the equatorial Atlantic than in the subtropics (40.5  
40 versus 41.0 Ma). We also show that, at both sites, the HO of *O. beckmanni* at 39.5 Ma  
41 is younger than published calibrations, increasing the duration of Zone E12 by at least  
42 400 kyr. In accordance with the tropical origins of *O. beckmanni*, this range  
43 expansion to higher latitudes may have occurred in response to sea surface warming  
44 during the MECO and subsequently disappeared with cooling of surface waters.

45

46 Keywords: Middle Eocene Climatic Optimum, Site 1051, Site 1260, planktonic  
47 foraminifera, biostratigraphy, magnetostratigraphy.

48

## 49 **1. Introduction**

50 Development of high-quality age models is essential for the reliable determination of

51 sequences of events in the geological record, i.e., a geological timescale, for  
52 correlation of palaeorecords between sites, and for estimating rates of change in  
53 palaeoenvironmental records. Construction of a reliable geological time scale for the  
54 middle Eocene has been hindered by a lack of high quality sedimentary sections. In  
55 part, these difficulties arise from a relatively shallow calcite compensation depth  
56 (CCD) in the Eocene compared to the modern day, which has resulted in  
57 comparatively poor preservation of contemporaneous carbonate microfossils in deep-  
58 sea sediments, particularly in the Pacific Ocean (Lyle et al., 2005). Weak  
59 palaeomagnetic signals typical of carbonate-rich Palaeogene sediments are a further  
60 complication for the calibration of biostratigraphic datums. Therefore, typically, deep-  
61 sea sections with good microfossil preservation are characterized by poor  
62 magnetostratigraphies (e.g., Ocean Drilling Program, ODP Legs 143, 154, 198 and  
63 208; Sager et al., 1993; Curry et al., 1995; Bralower et al., 2002; Zachos et al., 2004;),  
64 while those with good magnetostratigraphies suffer poor calcareous microfossil  
65 preservation (e.g., ODP Leg 199; Lyle et al., 2002). Similarly, in the classic land-  
66 based exposures in Italy (e.g., Gubbio) that constitute the magnetostratigraphic  
67 reference for a large part of the Eocene, calcareous microfossils are also typically  
68 poorly preserved and the magnetostratigraphy can be ambiguous (Lowrie et al., 1982;  
69 Napoleone et al., 1983; Jovane et al., 2007; Luciani et al., 2010).

70

71 One interval of Eocene time for which it has proven particularly problematic to obtain  
72 high quality sections (because of recovery difficulties), is the chron C18r/18n  
73 boundary and planktonic foraminiferal Zone E12 (Berggren and Pearson, 2005), the  
74 interval in which the MECO falls (Bohaty et al., 2009) (Fig. 1). Biozone E12 is  
75 defined by the total range of the short-lived tropical planktonic foraminiferal species

76 *Orbulinoides beckmanni*. *O. beckmanni* is a particularly useful biostratigraphic  
77 marker because, first, it divides what would otherwise be a long (~4 Myr) biozone,  
78 stretching from the highest occurrence (HO) of *Guembelitriones nuttalli* at 42.3 Ma to  
79 the HO of *Morozovelloides crassatus* at 38.0 Ma, Zones E11-E13 (Berggren and  
80 Pearson, 2005) (Fig. 1). Second, the existing calibration for Zone E12 is coincident  
81 with the MECO (Fig. 1) (Sexton et al., 2006a; Bohaty et al., 2009), which raises the  
82 possibility that *O. beckmanni* might represent an ‘excursion’ taxon akin to those  
83 documented for the Paleocene-Eocene Thermal Maximum (Kelly et al., 1996, 1998).  
84 However, the relatively poor recovery of Zone E12 by deep-sea drilling has hindered  
85 direct calibration of this Zone to the geomagnetic polarity time-scale (GPTS). A near  
86 global hiatus near the chron C18r/C18n boundary at ~40.0 Ma truncates the top of  
87 planktonic foraminiferal Zone E12 in many deep-sea sequences (e.g., Karig et al.,  
88 1975; Erbacher et al., 2004), while other sequences are limited by the presence of  
89 chert or condensation horizons (Zachos et al., 2004), a lack of carbonate (Lyle et al.,  
90 2002), poor magnetostratigraphic control or the absence of the marker species *O.*  
91 *beckmanni* (e.g., Sager et al., 1993; Curry et al., 1995; Bralower et al., 2002; Zachos  
92 et al., 2004).

93

94 Here we present new high-resolution magnetic polarity data from Site 1051 alongside  
95 quantitative records of the biostratigraphic marker species *O. beckmanni* and benthic  
96 foraminiferal stable isotope records from ODP Site 1051 and, for comparison, similar  
97 records from Site 1260 in the Atlantic Ocean. ODP Site 1051 represents an ideal  
98 section to address the above stratigraphic issues because, on the basis of available  
99 records, it has a high sedimentation rate for a deep-sea site in the middle Eocene (~4  
100 cm/kyr), it is stratigraphically continuous (at least to biozone and magnetostratigraphic

101 level), it hosts sediments that are suited to develop a resolvable magnetostratigraphy  
102 and it is situated well above the local CCD, favouring preservation of calcareous  
103 microfossils (Shipboard Scientific Party, 1998). For comparison, ODP Site 1260 also  
104 benefits from a good magnetostratigraphy and carbonate microfossil preservation, but  
105 the sedimentary succession is truncated by a hiatus at the chron C18r/18n boundary  
106 (Shipboard Scientific Party, 2004; Sugauma and Ogg, 2006). These new datasets are  
107 used to: (1) improve the magnetostratigraphic resolution of the late middle Eocene  
108 interval at Site 1051, (2) refine the existing biomagnetostratigraphic calibrations at  
109 Sites 1051 and 1260, (3) assess the chronological reliability of the bioevents that  
110 define Zone E12 at Sites 1051 and 1260, (4) test whether the MECO is present in  
111 these tropical and northern hemisphere sites and (5) determine if the speciation or  
112 subsequent extinction of *O. beckmanni* are linked to the MECO.

113

## 114 **2. Locations and geological setting**

115 ODP Site 1051 (30°03'N; 76°21'W, modern water depth 1980 meters below sea  
116 level, mbsl) is situated on the Blake Nose plateau in the western North Atlantic Ocean  
117 (Fig. 2). The estimated palaeodepth for Site 1051 is 1000 - 2000 mbsl for the middle  
118 Eocene (Shipboard Scientific Party, 1998) with a palaeolatitude of ~25°N (Ogg and  
119 Bardot, 2001). Site 1051 comprises a stratigraphically complete (at least to  
120 magnetochron level) expanded late Paleocene through middle Eocene sequence of  
121 siliceous nannofossil oozes interspersed with approximately 25 thin ash horizons  
122 (Shipboard Scientific Party, 1998). Estimated sedimentation rates are ~ 1 to 4 cm/kyr.

123

124 ODP Site 1260 (9°16'N; 54°33'W, modern water depth 2549 mbsl) (Fig. 2) was  
125 drilled on the Demerara Rise plateau (palaeowater depths for the Eocene close to

126 those of the present day, Arthur and Natland, 1979) and was situated at a  
127 palaeolatitude of 1°S in the middle Eocene (Suganuma and Ogg, 2006). Middle  
128 Eocene sediments at Site 1260 are primarily greenish grey nannofossil chalks with  
129 foraminifers and radiolarians (Shipboard Scientific Party, 2004), with average  
130 sedimentation rates across the focal interval of ~2 cm/kyr.

131

### 132 **3. Methods**

#### 133 *3.1 Palaeomagnetism*

134 To generate a continuous high-resolution magnetic polarity record across Zone E12  
135 at Site 1051, u-channel samples were taken following the shipboard composite depth  
136 section splice (Shipboard Scientific Party, 1998) between 66.15 and 146.63 meters  
137 composite depth (mcd). Below ~150 mcd, sediments were recovered using the  
138 extended core barrel, which makes them less suitable for detailed analysis.

139

140 All u-channel samples were measured on a 2-G Enterprises cryogenic magnetometer  
141 (at the National Oceanography Centre, Southampton) after progressive stepwise  
142 alternating field (AF) demagnetization at successive peak fields of 5, 10, 15, 20, 25,  
143 30, 40, 50 and 60 milliTesla (mT), and occasionally up to 80 mT. The natural  
144 remanant magnetization (NRM) was measured at 1 cm stratigraphic intervals,  
145 although smoothing occurs because of the width of the magnetometer response  
146 function (half-width = 5 cm). Thus, data from the top and bottom 5 cm of each u-  
147 channel were excluded from this study because of edge effects (Roberts, 2006). The  
148 inclination and declination of the characteristic remanant magnetization (ChRM) was  
149 determined at 1 cm intervals using principal component analysis; with data from at  
150 least 4 demagnetization steps, and the quality of the linear regressions was estimated

151 by calculating the maximum angular deviation associated with the best-fit line  
152 (Kirschvink, 1980). The age model for Site 1260 is based on Suganuma and Ogg  
153 (2006), which was supplemented by additional palaeomagnetic measurements by  
154 Edgar et al. (2007).

155

### 156 **3.2 *Orbulinoides beckmanni* abundance counts**

157 To determine the LO and HO of *Orbulinoides beckmanni*, high-resolution relative  
158 abundance counts (percent of total planktonic foraminifera) were produced for sample  
159 splits of ~400 individuals from 482 samples at 10 cm sampling resolution (mean  
160 sampling interval of 3 kyr) for ODP Site 1051 and on 69 samples at ~30 cm sampling  
161 resolution (sampling interval 12 kyr) at ODP Site 1260. Samples were prepared for  
162 abundance counts by washing 20 cm<sup>3</sup> of bulk sediment over a 63 µm mesh and then  
163 dry sieved at 300 µm. Biozonations and taxonomy adopted for this study are those of  
164 Berggren and Pearson (2005), and Proto-Decima and Bolli (1970) and Premoli Silva  
165 et al. (2006), respectively. We distinguish *O. beckmanni* from its immediate ancestor  
166 *Globigerinatheka euganea* (see Plates I and II) by the presence of spiral sutural  
167 apertures between early chambers (Plate IIb,f and h) and more numerous (>4) smaller,  
168 sutural apertures in the last few chambers, e.g., Plate II, specimens a,e, i, j and l. An  
169 additional diagnostic criterion is the presence of small, circular apertures within the  
170 wall of the last few large chambers (areal apertures; see Plate II, specimens a, c, i, j  
171 and l), commonly found in *O. beckmanni* but never reported in any of the  
172 globigerinathekids (Premoli-Silva et al., 2006). Thus, when present, areal apertures  
173 are a useful diagnostic characteristic.

174

### 175 **3.3 Oxygen and carbon isotope measurements**



176 Benthic foraminiferal stable isotope ( $\delta^{18}\text{O}$  and  $\delta^{13}\text{C}$ ) data were generated using the  
177 species *Cibicidoides eoceanus* (Site 1260) and *Oridorsalis umbonatus* (Site 1051),  
178 following taxonomy employed by Tjalsma and Lohmann (1983) and van Morkhoven  
179 et al. (1986). Foraminifera were picked from the size range 250-350  $\mu\text{m}$  and were  
180 cleaned by ultrasonication prior to isotopic analysis. Benthic foraminifera are  
181 relatively sparse at Site 1051 owing to dilution by siliceous microfossils. At Site 1260  
182 benthic foraminifera are more abundant and sufficient individuals for stable isotope  
183 analysis (~3-5) were found in every sample examined. All stable isotope  
184 measurements were determined using a Europa GEO 20-20 mass spectrometer  
185 equipped with an automatic carbonate preparation system (CAPS). Results are  
186 reported relative to the Vienna Pee Dee Belemnite (VPDB) standard with an external  
187 analytical precision of 0.07‰ and 0.03‰ for  $\delta^{18}\text{O}$  and  $\delta^{13}\text{C}$ , respectively. Stable  
188 isotope values generated from *Cibicidoides eoceanus* are adjusted to equilibrium by  
189 adding 0.28‰ VPDB to  $\delta^{18}\text{O}$  values, following the Palaeogene correction factor for  
190 *Cibicidoides* (Katz et al., 2003) and 0.72‰ VPDB is added to the  $\delta^{13}\text{C}$  values of  
191 *Oridorsalis umbonatus* to normalise to *Cibicidoides* (Katz et al., 2003).

192

## 193 **4. RESULTS**

### 194 ***4.1 Palaeomagnetic behavior and polarity zonation***

195 U-channel samples from Site 1051 have comparatively weak magnetizations ( $\sim 10^{-5}$  to  
196  $10^{-4} \text{ Am}^{-1}$ ), typical of carbonate-rich sediments, but with stable and readily interpreted  
197 palaeomagnetic behavior (Fig. 3a-f). Samples are characterized by a small, low-  
198 stability steeply dipping normal polarity component (Fig. 3a-f) that is interpreted to be  
199 as a drilling overprint. This magnetic overprint was successfully removed with peak  
200 AFs of <20 mT. The ChRM of the u-channel samples in the more strongly

201 magnetized composite section (108 – 146 mcd; Fig. 4) was isolated between 20 and  
202 50 mT and, toward the top of the composite section (~68 and 108 mcd), between the 5  
203 and 25 mT demagnetization steps (because of the less stable demagnetization  
204 behavior in this upper interval, Fig. 3g and h). This is not ideal, and particular care  
205 was taken to discard data in this interval if there was a suggestion of an unremoved  
206 drilling overprint.

207

208 Magnetic polarity intervals were determined based on the clustering of positive or  
209 negative inclinations. Our new data from between 65 and 150 mcd provide a  
210 substantial improvement on the published lower-resolution dataset available between  
211 0 and 150 mcd (Shipboard Scientific Party, 1998; Ogg and Bardot, 2001) (Fig. 4).  
212 Five distinct magnetozones (R1 to R3) are identified (Fig. 4), in our new dataset and  
213 the boundaries between these improved from a previous resolution of  $\pm 2.5$  m (Ogg  
214 and Bardot, 2001) to between  $< 2$  cm and  $\sim 1$  m (Table 1).

215

216 Within each of the ‘long’ magnetozones investigated (N1 through N2) are a number  
217 of short-lived ( $\sim 2$ -8 kyr) polarity intervals, e.g., at 128 and 130 mcd (Fig. 4). The  
218 majority of these short-lived polarity features are associated with large increases in  
219 the measured NRM intensity (Fig. 4) and are likely to reflect measurement artifacts  
220 resulting from large changes in NRM intensity (Roberts, 2006). These features might  
221 be attributable to dispersed ash particles that are coincident with at least several of the  
222 polarity events. One notable exception to this pattern occurs at 100 mcd (Fig. 4),  
223 which might represent an example of a short polarity interval associated with ‘tiny  
224 wiggles’ (e.g., Roberts and Lewin-Harris, 2000) that are observed in seafloor  
225 magnetic anomaly profiles within the late middle Eocene (Cande and Kent, 1992).

226 Regardless, the short-lived polarity intervals identified here are not considered in the  
227 overall polarity zonation.

228

#### 229 ***4.2 Planktonic foraminiferal biostratigraphy***

230 Planktonic foraminiferal assemblages at Sites 1051 and 1260 are typical of those  
231 found in (sub)tropical oceans in the late middle Eocene and are indicative of  
232 planktonic foraminiferal Zones E11 through E13. Microfossil preservation is good  
233 with planktonic foraminifera showing some evidence of recrystallization; specimens  
234 are ‘frosty’, not ‘glassy’ (Sexton et al., 2006b).

235

236 We have identified *Orbulinoides beckmanni* at both ODP sites (Table 2). *O.*  
237 *beckmanni* has some morphological variability within its range, with a shift to a more  
238 encompassing final chamber (increased test sphericity) and an increasing number of  
239 small supplementary sutural apertures at the base of the final chamber and between  
240 the earlier chambers (Plates I and II). This leads to highly distinctive forms toward the  
241 top of its stratigraphic range (Plate II). Of note, we find no stratigraphic significance  
242 in the presence or absence of areal apertures or ‘bulla-like’ structures.

243

244 The relative abundance of *O. beckmanni* within the total planktonic foraminiferal  
245 assemblage is shown in Figure 5a and b. Using our new magnetic stratigraphy for  
246 subtropical ODP Site 1051, we determine the LO of *O. beckmanni* to 40.5 Ma using  
247 the geomagnetic polarity time scale of Cande and Kent (1992, 1995; Fig. 5a), in the  
248 upper half of chron C18r (106.15 mcd). At equatorial Site 1260, the LO of *O.*  
249 *beckmanni* occurs toward the base of chron C18r (58.87 mcd) around a half million  
250 years earlier (41.0 Ma, Fig. 5b).

251

252 At both sites, for several hundred thousand years following its LO, *O. beckmanni*  
253 remains low in relative abundance (<2%, Fig. 5). At Site 1051, where a longer record  
254 is available, an abrupt increase (to ~4-6%) in the relative abundance of *O. beckmanni*  
255 occurs toward the base of chron C18n.2n at 40.1 Ma. Its relative abundance then  
256 remains on average at 3% for approximately 600 kyr, followed by a decrease and  
257 eventual extinction of *O. beckmanni* within chron C18n.1n at 61.90 mcd (at 39.5 Ma).  
258 We are unable to identify the HO of *O. beckmanni* at Site 1260 because the  
259 sedimentary succession is truncated by a hiatus at 36.1 mcd, which spans  
260 approximately five million years of geological time (middle-late Eocene) (Shipboard  
261 Scientific Party, 2004).

262

### 263 ***4.3 Stable isotope records***

264 At both sites, benthic foraminiferal  $\delta^{18}\text{O}$  records gradually shift by ~1‰ to lower  
265 values within chron C18r coincident with an overall shift to higher  $\delta^{13}\text{C}$  values (Fig.  
266 5c and d). The stable isotope record at Site 1260 is truncated by a hiatus at the top of  
267 chron C18r, but at Site 1051, benthic  $\delta^{18}\text{O}$  values reach a short-lived (~40 kyr)  
268 minimum in the base of chron C18n.2n (at 40.05 Ma) coincident with an abrupt 1‰  
269 decrease in  $\delta^{13}\text{C}$  values (Fig. 5). Subsequently, both benthic  $\delta^{18}\text{O}$  and  $\delta^{13}\text{C}$  values at  
270 Site 1051 increase rapidly, followed by a more gradual shift to overall higher values.  
271 There is good agreement between the amplitude and timing of the  $\delta^{18}\text{O}$  shift in the  
272 bulk (Bohaty et al., 2009) and benthic  $\delta^{18}\text{O}$  records (this study) at Site 1051. At Site  
273 1260, superimposed on the longer-term patterns of stable isotope change are a number  
274 of discrete negative  $\delta^{13}\text{C}$  excursions (~1‰) with a duration of ~40 kyr each at 40.3,  
275 40.4, 41.2 and 41.4 Ma (Fig. 5d). The two oldest of these four excursions, occur prior

276 to the onset of the MECO and are not associated with any obvious lithological  
277 changes (Shipboard Scientific Party, 2004). In contrast, the younger  $\delta^{13}\text{C}$  excursions  
278 at 40.3 and 40.4 Ma, superimposed on the shift to more positive  $\delta^{13}\text{C}$  values during  
279 the MECO are coincident with thin (1-2 cm thick) clay horizons (cf. the C19r event  
280 already documented at Site 1260, Edgar et al. 2007). None of these  $\delta^{13}\text{C}$  excursions  
281 are readily discernible in the lower-resolution benthic  $\delta^{13}\text{C}$  record of Site 1051 (Fig.  
282 5d).

283

## 284 5. Discussion

### 285 *5.1 Correlation to the Geomagnetic Polarity Time Scale*

286 We integrate our new magnetic polarity pattern with published datasets (Shipboard  
287 Scientific Party, 1998; Ogg and Bardot, 2001) between 0 and 150 mcd identifying  
288 nine distinct magnetozones (R1-N4; Fig. 6). The resulting polarity patterns provides a  
289 correlation with the GPTS between chrons C19r and C17r (Fig. 6). From 150 to 90  
290 mcd our interpretation is in good agreement with published records (Shipboard  
291 Scientific Party, 1998; Ogg and Bardot, 2001). However, above 90 mcd our  
292 interpretation differs from that of the Shipboard Scientific Party (1998) and Ogg and  
293 Bardot (2001) significantly, resulting in a two million year offset (Fig. 6). This  
294 discrepancy arises from our differentiation of chron C18 into subchrons C18n.2n,  
295 C18n.1r and C18n.1n, leading to the re-assignment of magnetozone N2 to chron  
296 C18n.2n, and of subsequent chrons, e.g., magnetozone R3 = chron C18n.1r, N3 =  
297 chron C18n.1n, R4 = chron C17r and N4 = chron C17n. Chron C18n was not  
298 differentiated in the earlier polarity scheme because interpretation of the polarity  
299 pattern based on calcareous nannofossil datums suggested that C18n was very  
300 condensed at this site (Fig. 6, Shipboard Scientific Party, 1998; Ogg and Bardot,

301 2001). Resulting sedimentation rates for Site 1051 are relatively uniform (~4 cm/kyr)  
302 and are consistent with planktonic foraminiferal and radiolarian datums (Fig. 6).  
303 However, existing age calibrations for the respective HO and LO of calcareous  
304 nannofossil taxa *Dictyococcites bisectus* and *Chiasmolithus oamaruensis* are offset by  
305 almost one million years from the new age model (Fig. 6) and indicate the need for  
306 further calibration of biostratigraphic datums to the GPTS.

307

### 308 ***5.2 Revised calibrations for the lowest and highest occurrence of Orbulinoides*** 309 ***beckmanni***

310 At Site 1051, high sedimentation rates, good magnetostratigraphic control and high-  
311 resolution sampling allow us to directly calibrate the LO and HO of *Orbulinoides*  
312 *beckmanni* to the GPTS. Using our new age model for Site 1051, and the published  
313 refined magnetic stratigraphy from Site 1260 (Suganuma and Ogg, 2006; Edgar et al.,  
314 2007), a 500 kyr offset is evident in the position of the LO of *O. beckmanni* between  
315 Sites 1051 and 1260 (Fig. 5a and b). While the LO of *O. beckmanni* at Site 1051 in  
316 chron C18r (40.5 Ma) is consistent with that indicated by Berggren et al. (1995), at  
317 Site 1260 it is earlier (at the base of chron C18r at 41.0 Ma). The diachroneity  
318 reported here exceeds the uncertainties that are reasonably attributable to  
319 methodological ( $\pm < 13$  kyr) or age model inconsistencies ( $\pm < 38$  kyr) and is therefore  
320 interpreted to represent genuine geological diachrony between the two Atlantic Ocean  
321 sites of ~500 kyr. Consistent with the latitudinal diachrony observed between 2°S  
322 (Site 1260) and 25°N (Site 1051) is the later LO of *O. beckmanni* reported at  
323 40.2±0.04 Ma (in the top part of chron C18r) at ~40°N in the Contessa Highway  
324 section, Italy (Jovane et al., 2007) (Fig 2). Recognition of the regionally diachronous  
325 LO of *O. beckmanni* has probably gone undetected previously because of the lack of

326 sections available on which the LO and HO can be tied directly to the GPTS.

327

328 Of note, the HO of *O. beckmanni* recorded here at Site 1051 in magnetochron  
329 C18n.1n is much later (600 kyr) than that reported in a recent calibration of its HO to  
330 40.0 Ma in chron C18n.2n at ODP Site 1052 (Wade, 2004). This discrepancy is most  
331 likely attributable to the equivocal recognition and subdivision of chron C18n at Site  
332 1052 (Ogg and Bardot, 2001), and is further complicated by the proposal of a 600  
333 kyr-long hiatus (Pälike et al., 2001). Because the LO and HO of *O. beckmanni* defines  
334 the upper and lower boundaries of planktonic foraminiferal Zone E12, this zone at  
335 Site 1051 is at least 400 kyr longer than existing calibrations (Berggren and Pearson,  
336 2005).

337

### 338 **5.3 Environmental controls on *Orbulinoides beckmanni*'s biogeography**

339 We invoke an environmental control on the biogeography of *O. beckmanni* to explain  
340 the observed diachroneity in its lowest occurrence and its short total range duration.  
341 Expansion of species ranges from the tropics to higher latitudes is a common source  
342 of diachrony in first appearances of marine plankton (Kennett, 1970; Moore et al.,  
343 1993; Raffi et al., 1993; Spencer-Cervato et al., 1994; Kucera and Kennett, 2000;  
344 Sexton and Norris, 2008). Although little is known about the palaeoecology of *O.*  
345 *beckmanni*, this species is restricted to tropical and warm mid-latitudes (Bolli et al.,  
346 1972; Premoli Silva et al., 2006;) between ~30°S and 45°N, highlighted in our  
347 compilation of geographic occurrence (Fig. 2), suggesting that sea surface  
348 temperature (SST) may have played a major role in its geographic distribution. As  
349 surface waters warmed during the MECO (Bohaty and Zachos, 2003; Bohaty et al.,  
350 2009), conditions may have become more favorable for this taxon at higher latitudes

351 thereby allowing geographic range expansion to  $\sim 45^\circ\text{N}$  (Fig. 2).

352

353 The HO of *O. beckmanni* post-dates the MECO at Site 1051 by at least 600 kyr (Fig.  
354 5) which indicates that the apparent abrupt cooling at the termination of the MECO  
355 was not sufficient to completely eliminate this species from Site 1051. However, SST  
356 continued to decrease (Bohaty et al., 2009) and may have fallen below a critical  
357 threshold necessary to sustain viable population numbers. Despite the undoubted  
358 diagenetic overprint on the bulk sediment record,  $\delta^{18}\text{O}$  values at the LO and HO of *O.*  
359 *beckmanni* are similar ( $\sim 0.7\text{‰}$ , Fig. 5c), which is compatible with a thermal threshold  
360 controlling *O. beckmanni*'s distribution. This also raises the possibility that the HO of  
361 *O. beckmanni* may be latitudinally diachronous. This interpretation is in keeping with  
362 the earlier HO of *O. beckmanni* (39.9 Ma, base of chron C18n.2n) at  $40^\circ\text{N}$  in the  
363 Contessa section (Jovane et al., 2007; Fig. 2). *O. beckmanni* is not confined to the  
364 MECO event and thus, by definition, this species cannot be termed an 'excursion  
365 taxon'. Nevertheless, the relatively short range of *O. beckmanni* ( $<1$  Myr), combined  
366 with the coincidence of its peak abundance with peak ocean warmth, implies that this  
367 taxon had a narrow environmental tolerance and/or the ecological niche that it  
368 occupied disappeared because of cooling surface waters (Fig. 5c).

369

#### 370 **5.4 Constraints on the timing and environmental impact of the MECO**

371 Our correlation of the magnetostratigraphic records to the GPTS suggests that the  
372 transient  $\delta^{18}\text{O}$  and  $\delta^{13}\text{C}$  shifts observed across the chron C18r/18n boundary at Sites  
373 1260 and 1051 (Fig. 5c and d) are low latitude representations of the MECO. These  
374 are the first detailed records from the (sub)tropics and demonstrate that the MECO is  
375 a truly global event. The magnitude, relative timing and pattern of stable isotope



376 change are consistent with published benthic foraminiferal (e.g., ODP Site 748, Fig.  
377 5c; Bohaty and Zachos, 2009) and bulk sediment (Jovane et al., 2007; Bohaty et al.,  
378 2009; Spofforth et al., 2010) stable isotope records from other ocean basins, which  
379 implies that the gradual onset and abrupt  $\delta^{18}\text{O}$  maximum are reliable for global  
380 stratigraphic correlation (Fig. 5c and d).

381

382 At present it is unclear whether the higher-resolution features, notably, the two  $\delta^{13}\text{C}$   
383 excursions preceding the MECO peak at Site 1260, are also global in character.  
384 Because these excursions are coincident with clay layers which imply carbonate  
385 dissolution, they are reminiscent of simultaneous transient CCD shoaling and negative  
386 isotopic shifts associated with small inferred 'hyperthermal' events reported in other  
387 parts of the Eocene (e.g., Lourens et al., 2005; Edgar et al., 2007; Quillévéré et al.,  
388 2008). If these excursions prove to be present in other deep-sea sites, they may help to  
389 shed light on the mechanisms driving warming during the MECO.

390

## 391 **6. Conclusions**

392 We present new stable isotopic, magnetostratigraphic, and biostratigraphic records  
393 from (sub)tropical Atlantic ODP Sites 1051 and 1260 for the late middle Eocene,  
394 spanning the MECO. These represent the first detailed records of the MECO from the  
395 tropics and subtropics and demonstrate that the event is truly global. Closely  
396 associated with the MECO is the range and abundance variations of the  
397 biostratigraphically important planktonic foraminiferal species *O. beckmanni*.  
398 Detailed abundance counts of this species reveal a latitudinal diachrony of ~500 kyrs  
399 in its lowest occurrence, observed 500 kyrs earlier in the tropics (41.0 Ma at Site  
400 1260) than in the subtropics (40.5 Ma at Site 1051). This latitudinal diachrony is

401 attributed to the poleward expansion of warm surface waters during the onset of the  
402 MECO, which created favorable conditions at extra-tropical latitudes for this  
403 thermophillic species. Using our high-resolution magnetic polarity record at ODP  
404 Site 1051, the diachronous FO of *O. beckmanni* occurs within chron C18r and its  
405 disappearance within chron C18n.1n at 39.5 Ma, 600 kyr younger than previously  
406 reported. The disappearance of *O. beckmanni* from the subtropics is likely related to  
407 progressive cooling of sea surface waters below some critical threshold rather than to  
408 abrupt environmental change.

409

#### 410 **Acknowledgements**

411

412 We thank M. Bolshaw, G. Paterson, R. Pearce and D. Spanner for help with  
413 laboratory work, and S. Bohaty for access to stable isotope data from ODP Sites 748  
414 and 1051. Bridget Wade and an anonymous reviewer are thanked for their  
415 constructive reviews of this manuscript. Financial support was provided by a NERC  
416 small grant to SJG and PAW, a NERC CASE studentship (with Perkin Elmer) to  
417 KME and a NERC UKIODP Rapid Response Grant to PFS. This work used samples  
418 provided by the Ocean Drilling Program (ODP). The ODP (now IODP) is sponsored  
419 by the US National Science Foundation and participating countries under the  
420 management of the Joint Oceanographic Institutions (JOI), Inc.

421

#### 422 **References**

423

424 Arthur, M.A. and Natland, J.H., 1979. Carbonaceous sediments in the North and  
425 South Atlantic: The role of salinity in stable stratification of Early Cretaceous basins.

426 In: Talwani, M.E.A. (Ed.), Deep Drilling Results in the Atlantic Ocean: Continental  
427 Margins and Palaeoenvironment. American Geophysical Union, Maurice Ewing  
428 Series 3, pp. 375-401.

429

430 Babic, L., Kußenjak, M.H., Coric, S. and Zupanic, J., 2007. The middle Eocene age of  
431 the supposed late Oligocene sediments in the flysch of the Pazin Basin (Istria, Outer  
432 Dinarides). Croatian Natural History Museum 16, 83-103.

433

434 Berggren, W.A., Kent, D.V., Swisher, C. and Aubry, M.-P., 1995. A revised Cenozoic  
435 geochronology and chronostratigraphy. In: Berggren, W.A., Kent, D.V., Aubrey, M.-  
436 P. and Hardenbol, J. (Eds.), Geochronology, Time-Scales and Global Stratigraphic  
437 Correlation. Tulsa, SEPM Special Publication 54, pp. 129-212.

438

439 Berggren, W.A. and Pearson, P.A., 2005. A revised tropical to subtropical planktonic  
440 foraminiferal zonation of the Eocene and Oligocene. Journal of Foraminiferal  
441 Research 35, 279-298.

442

443 Bohaty, S.M. and Zachos, J.C., 2003. Significant Southern Ocean warming in the late  
444 middle Eocene. Geology 31, 1017-1020.

445

446 Bohaty, S.M., Zachos, J.C., Florindo, F. and Delaney, M.L., 2009. Coupled  
447 greenhouse warming and deep-sea acidification in the middle Eocene.  
448 Paleoceanography 24, PA2207 doi:10.1029/2008PA001676.

449

450 Bolli, H.M., 1972. The genus *Globigerinatheka* Brönnimann. Journal of Foraminiferal

451 Research 2, 109-136.

452

453 BouDagher-Fadel, M. and Clark, G.N., 2006. Stratigraphy, palaeoenvironment and  
454 palaeogeography of Maritime Lebanon: a key to Eastern Mediterranean Cenozoic  
455 history. *Stratigraphy* 3, 81-118.

456

457 Bralower, T.J., Premoli Silva, I., Malone, M.J., et al., 2002. Proceedings of the Ocean  
458 Drilling Program Initial Reports 198. College Station, Texas (Ocean Drilling  
459 Program).

460

461 Cande, S.C. and Kent, D.V., 1992. A new geomagnetic polarity time scale for the  
462 Late Cretaceous and Cenozoic. *Journal of Geophysical Research* 97, 13917-13951.

463

464 Cande, S.C. and Kent, D.V., 1995. Revised calibration of the geomagnetic polarity  
465 timescale for the Late Cretaceous and Cenozoic. *Journal of Geophysical Research*  
466 100, 6093-6095.

467

468 Curry, W.B. Shackleton, N.J., Richter, C., et al., 1995. Proceedings of the Ocean  
469 Drilling Program Initial Reports, 154. College Station, Texas (Ocean Drilling  
470 Program).

471

472 Edgar, K.M., Wilson, P.A., Sexton, P.F. and Suganuma, Y., 2007. No extreme bipolar  
473 glaciation during main Eocene compensation shift. *Nature* 448, 908-911.

474

475 Gradstein, F.M., Ogg, J.G. and Smith, A.G., 2004, *A Geologic Time Scale 2004*.

476 Cambridge University Press.

477

478 Jovane, L., Florindo, F., Coccioni, R., Dinarès-Turell, J., Marsili, A., Monechi, S.,  
479 Roberts, A.P. and Sprovieri, M., 2007. The middle Eocene climatic optimum event in  
480 the Contessa Highway section, Umbrian Apennines, Italy. *Geological Society of*  
481 *America Bulletin* 119, 413-427.

482

483 Karig D.E., Ingle, J.C.Jr., et al., 1975. Initial Reports of the Deep Sea Drilling Project  
484 31, Washington (U.S. Government Printing Office).

485

486 Katz, M.E., Katz, D.R., Wright, J.D., Miller, K.G., Pak, D.K., Shackleton, N.J. and  
487 Thomas, E., 2003. Early Cenozoic benthic foraminiferal isotopes: species reliability  
488 and interspecies correction factors. *Paleoceanography* 18, 1024, doi:  
489 10.1029/2002PA000798.

490

491 Kelly, D.C., Bralower, T.J., Zachos, J.C., Premoli-Silva, I. and Thomas, E., 1996.  
492 Rapid diversification of planktonic foraminifera in the tropical Pacific (ODP Site 865)  
493 during the latest Paleocene thermal maximum. *Geology* 24, 423-426.

494

495 Kelly, D.C., Bralower, T.J., Zachos, J.C., 1998. Evolutionary consequences of the  
496 latest Paleocene thermal maximum for tropical planktonic foraminifera.  
497 *Palaeogeography, Palaeoclimatology, Palaeoecology* 141, 139-161.

498

499 Kennett, J.P., 1970, Pleistocene palaeoclimates and foraminiferal biostratigraphy in  
500 subantarctic deep-sea cores: *Deep-Sea Research, A*, 17, 125–140.

501

502 Kirschvink, J.L., 1980. The least-squares line and plane and line analysis of  
503 palaeomagnetic data. *Geophysical Journal of the Royal Astronomical Society* 62, 699-  
504 718.

505

506 Kucera, M. and Kennett, J.P., 2000. Biochronology and evolutionary implications of  
507 Late Neogene California margin planktonic foraminiferal events. *Marine*  
508 *Micropalaeontology* 40, 67-81.

509

510 Lowrie, W., Alvarez, W., Napoleone, G., Perch-Nielson, K., Premoli Silva, I. and  
511 Tomarkine, M., 1982. Palaeogene magnetic stratigraphy in Umbrian pelagic  
512 carbonate rocks: the Contessa sections, Gubbio. *Geological Society of America*  
513 *Bulletin* 93, 414-432.

514

515 Luciani, V., Giusberti, L., Agnini, C., Fornaciari, E., Rio, D., Spofforth, D.J., Pälike,  
516 2010. Ecological and evolutionary response of tethyan planktonic foraminifera to the  
517 middle Eocene climatic optimum (Meco) from the Alano section (NE Italy).  
518 *Palaeogeography, Palaeoclimatology, Palaeoecology* 292, 82-95.

519

520 Lyle, M., Wilson, P.A., Janecek, T.R. et al., 2002. *Proceedings of the Ocean Drilling*  
521 *Program Initial Reports* 199. College Station, Texas (Ocean Drilling Program).

522

523 Lyle, M., Olivarez-Lyle, A., Backman, J. and Tripathi, A., 2005. Biogenic  
524 sedimentation in the Eocene equatorial Pacific – the stuttering greenhouse and Eocene  
525 compensation depth. In: Wilson, P.A., Lyle, M. and Firth, J.V. (Eds.), *Proceedings of*

526 the Ocean Drilling Program Scientific Results 199. College Station, Texas (Ocean  
527 Drilling Program), doi:10.2973/odp.proc.sr.199.219.2005.

528

529 Moore, T.C., Shackleton, N.J. and Pisias, N.G., 1993. Paleooceanography and the  
530 diachrony of radiolarian events in the eastern equatorial Pacific. *Paleoceanography* 8,  
531 567-586.

532

533 Napoleone, G., Premoli Silva, I., Heller, F., Cheli, P., Corezzi, S. and Fischer, A.F.,  
534 1983. Eocene magnetic stratigraphy at Gubbio, Italy, and its implications for  
535 Palaeogene geochronology. *Geological Society of America Bulletin* 94, 181-191.

536

537 Norris, R.D., Kroon, D., Klaus, A. et al., 1998. Proceedings of the Ocean Drilling  
538 Program Initial Reports 171B. College Station, Texas (Ocean Drilling Program).

539

540 Ogg, J.G. and Bardot, L., 2001. Aptian through Eocene magnetostratigraphic  
541 correlation of the Blake Nose Transect (Leg 171B), Florida continental margin. In:  
542 Kroon, D., Norris, R.D., and Klaus, A. (Eds.), Proceedings of the Ocean Drilling  
543 Program Scientific Results 171B: College Station, Texas (Ocean Drilling Program),  
544 doi:10.2973/odp.proc.sr.171b.104.2001.

545

546 Pälike, H., Shackleton, N.J. and Röhl, U., 2001, Astronomical forcing in late Eocene  
547 marine sediments. *Earth and Planetary Science Letters* 193, 589-602.

548

549 Premoli Silva, I., Wade, B.S. and Pearson, P.N., 2006, Taxonomy of Globigerinatheka  
550 and Orbulinoides. In: Pearson, P.N., Olsson, R.K., Huber, B.T., Hemleben, C. and

- 551 Berggren, W.A. (Eds.), Atlas of Eocene Planktonic Foraminifera. Cushman  
552 Foundation Special Publication, 41, pp. 169-212.  
553
- 554 Proto Decima, F. and Bolli, H., 1970. Evolution and variability of *Orbulinoides*  
555 *beckmanni* (Saito). *Eclogae Geologicae Helvetiae*. 63, 883-905.  
556
- 557 Raffi, I., Backman, J., Rio, D. and Shackleton, N.J., 1993. Plio-Pleistocene  
558 nannofossil biostratigraphy and calibration to oxygen isotope stratigraphies from  
559 Deep Sea Drilling Project Site 607 and Ocean Drilling Program Site 677.  
560 *Paleoceanography* 8, 387-403.  
561
- 562 Roberts, A.P., 2006. High-resolution magnetic analysis of sediment cores: strengths,  
563 limitations and strategies for maximizing the value of long-core magnetic data.  
564 *Physics of the Earth and Planetary Interiors*, 156, 162-178.  
565
- 566 Roberts, A.P. and Lewin-Harris, J.C., 2000, Magnetic marine anomalies: evidence  
567 that 'tiny wiggles' represent short-period geomagnetic polarity intervals, *Earth and*  
568 *Planetary Science Letters*, 183, 375-388.  
569
- 570 Sager, W.W., Winterer, E.L., Firth, J.V., et al., 1993, *Proceedings of the Ocean*  
571 *Drilling Program Initial Reports* 143. College Station, Texas (Ocean Drilling  
572 Program).  
573
- 574 Schrag, D.P., Depaolo, D.J. and Richter, F.M., 1995, Reconstructing past sea-surface  
575 temperatures - correcting for diagenesis of bulk marine carbonate, *Geochimica et*



576 Cosmochimica Acta, 59, 2265-2278.

577

578 Sexton, P.F., Wilson, P.A. and Norris, R.D., 2006a, Testing the Cenozoic multisite  
579 composite  $\delta^{18}\text{O}$  and  $\delta^{13}\text{C}$  curves: new monospecific Eocene records from a single  
580 locality, Demerara Rise (Ocean Drilling Program Leg 207), Paleoceanography, 21,  
581 PA2019, doi:10.1029/2005PA001253.

582

583 Sexton, P.F., Wilson, P.A. and Pearson, P.N., 2006b, Microstructural and  
584 geochemical perspectives on planktic foraminiferal preservation: “glassy” versus  
585 “frosty”. Geochemistry, Geophysics, Geosystems 7, Q12P19,  
586 doi:10.1029/2006GC001291.

587

588 Sexton, P.F., and Norris, R.D. 2008, Dispersal and biogeography of marine plankton:  
589 long-distance dispersal of the foraminifer *Truncorotalia truncatulinoides*, Geology,  
590 36, 899-902.

591

592 Shipboard Scientific Party, 1998. Site 1051. In: Norris, R.D., Kroon, D., Klaus, A. et  
593 al., (Eds.), Proceedings of the Ocean Drilling Program Initial Reports 171B. College  
594 Station, Texas (Ocean Drilling Program).

595

596 Shipboard Scientific Party, 2004. Site 1260. In: Erbacher, J., Mosher, D.C., Malone,  
597 M.J. et al. (Eds.), Proceedings of the Ocean Drilling Program Initial Reports 207.  
598 College Station, Texas (Ocean Drilling Program).

599

600 Spencer-Cervato, C., Thiersten, H.R., Lazarus, D.B. and Beckmann, J-P., 1994. How

- 601 synchronous are Neogene marine plankton events? *Paleoceanography* 9, 739-763.
- 602
- 603 Saganuma, Y. and Ogg, J.G., 2006. Campanian through Eocene magnetostratigraphy  
604 of Sites 1257-1261, ODP Leg 207, Demerara Rise (western equatorial Atlantic). In:  
605 Mosher, D.C., Erbacher, J. and Malone, M.J. (Eds.), *Proceedings of the Ocean*  
606 *Drilling Program Scientific Results 207: College Station, Texas (Ocean Drilling*  
607 *Program)*.
- 608
- 609 Tjalsma, R.C. and Lohmann, G.P., 1983. Paleocene-Eocene bathyal and abyssal  
610 benthic foraminifera from the Atlantic Ocean. *Micropalaeontology Special*  
611 *Publication 4*.
- 612
- 613 van Morkhoven, F.P.C.M., Berggren, W.A. and Edwards, A.S., 1986. Cenozoic  
614 cosmopolitan deep-water benthic foraminifera. *Elf-aquitaine, Pau*.
- 615
- 616 Wade, B.S., 2004. Planktonic foraminiferal biostratigraphy and mechanisms in the  
617 extinction of *Morozovella* in the late middle Eocene. *Marine Micropalaeontology* 51,  
618 23-38.
- 619
- 620 Zachos, J.C., Kroon, D., Blum, P., et al., 2004. *Proceedings of the Ocean Drilling*  
621 *Program Initial Reports 208. College Station, Texas (Ocean Drilling Program)*.
- 622
- 623 Zachos, J.C., Dickens, G.R. and Zeebe, R.E., 2008. An early greenhouse perspective  
624 on greenhouse warming and carbon-cycle dynamics. *Nature* 451,  
625 doi:10.1038/nature06588.

626

627 **Figure captions**

628

629 Figure 1 – Study interval in the context of Cenozoic climate trends. a) Cenozoic  
630 benthic foraminiferal  $\delta^{18}\text{O}$  record modified from Zachos et al. (2008). The MECO is  
631 shown on a revised age scale in keeping with this study. b) The Geomagnetic polarity  
632 time scale used follows Cande and Kent (1992; 1995). New ‘E’ planktonic  
633 foraminiferal tropical biozonation scheme from Berggren and Pearson (2005), and ‘P’  
634 tropical biozonation scheme from Berggren et al. (1995). c) Benthic foraminiferal  
635  $\delta^{18}\text{O}$  record from Site 748, Southern Ocean (Bohaty et al., 2009). Black vertical line  
636 represents the duration of the MECO based on the  $\delta^{18}\text{O}$  stable isotope pattern. Black  
637 dashed lines denote the position of the MECO relative to the GPTS and tropical  
638 zonation scheme. Grey boxes denote the study interval and the black vertical line  
639 represents the duration of the MECO based on the  $\delta^{18}\text{O}$  pattern.

640

641 Figure 2 – Palaeogeographic reconstruction of the Eocene illustrating the presence  
642 and absence of *Orbulinoides beckmanni*. ODP Sites 1051 and 1260 (stars) used in this  
643 study. Solid circles indicate the presence and open circles the absence of *O.*  
644 *beckmanni*. Data are compiled from deep-sea drill sites and exposed marine sections  
645 that coincide with planktonic foraminiferal Zone E12 but are not necessarily  
646 stratigraphically ‘complete’ sections. Data are compiled from Lowrie et al. (1982),  
647 BouDagher-Fadel and Clark (2006), Pearson et al. (2006), Babic et al. (2007), Jovane  
648 et al. (2007) and <http://www-odp.tamu.edu/database/>. To prevent bias, sites where *O.*  
649 *beckmanni* is absent because of hiatuses, dissolution, lack of carbonate or non-  
650 recovery of this stratigraphic interval are excluded. The base map for 40 Ma was

651 generated from [www.odsn.de/odsn/series/palaeomap/palaeomap.html](http://www.odsn.de/odsn/series/palaeomap/palaeomap.html).

652

653 Figure 3 – Typical AF (alternating field) demagnetization behavior of sediments from  
654 ODP Site 1051. a-f) samples with stable demagnetization behaviour. g-h) samples  
655 with less-stable demagnetization behaviour. In the vector component diagrams, open  
656 symbols represent projections onto the vertical plane and closed onto the horizontal  
657 plane.  $J_{max}$  is the NRM value measured during AF demagnetization.

658

659 Figure 4 – Down-core variations in the intensity of the natural remanent  
660 magnetization (NRM) and inclination for ODP Site 1051. a) Inclination data from  
661 Ogg and Bardot (2001). Closed symbols represent data points with maximum angular  
662 deviation (MAD) values of  $<10^\circ$ , while open data points have MAD values between  
663  $10^\circ$  and  $15^\circ$ . b) MAD values of data shown in panels c and d. c) NRM intensity after  
664 AF demagnetization at 25 mT for samples shown in panel c. d) Inclination data for the  
665 shipboard composite depth sections (mcd – meters composite depth). Grey symbols =  
666 data from Hole A and black symbols from Hole B, with MAD values of  $<10^\circ$  (this  
667 study). Horizontal dashed lines represent splice points. The magnetic polarity  
668 zonation is shown on the right. Black represents normal and white represents reversed  
669 polarity intervals.

670

671 Figure 5 – Stable isotope records across the middle Eocene climatic optimum and  
672 relative abundance records of *O. beckmanni*. Relative abundance records of *O.*  
673 *beckmanni* at ODP Sites 1051 (panel a) and 1260 (panel b). Horizontal black lines  
674 denote core depths between which the lowest and highest occurrences (LO and HO)  
675 of *O. beckmanni* were recorded by the Shipboard Scientific Parties (1998; 2004).

676 Revised planktonic foraminiferal zone boundaries based on this study shown. Arrows  
677 indicate new placement of the boundaries of Zone E12. c) Benthic foraminiferal  $\delta^{18}\text{O}$   
678 records from Sites 1051 and 1260 (this study). Starred (\*) records are from Bohaty et  
679 al. (2009) and are aligned on the new Site 1051 age model. d) Benthic foraminiferal  
680  $\delta^{13}\text{C}$  records from Sites 1051 and 1260 (this study). Starred (\*) records are from  
681 Bohaty et al. (2009) and are aligned on the new Site 1051 age model.

682

683 Figure 6 - Age versus depth plot with correlation of the ODP Site 1051 polarity  
684 zonation to the geomagnetic polarity time scale of Cande and Kent (1992, 1995).  
685 Calcareous plankton and radiolarian datums determined by the Shipboard Scientific  
686 Party (1998) are shown by colored diamonds (errors indicated by vertical black lines).  
687 Ages are from Berggren et al. (1995), with the exception of the highest occurrence  
688 (HO) of *O. beckmanni* and the extinction of *Morozovelloides* and large acarininids,  
689 which are from Wade (2004). Revised placement of the LO and HO of *O. beckmanni*  
690 are shown by solid circles. Polarity intervals marked 'R' have reversed polarity and  
691 those marked 'N' have normal polarity. mcd = metres composite depth. The grey line  
692 represents the age model from SSP'98 = Shipboard Scientific Party (1998) and  
693 O&B'01 = Ogg and Bardot (2001).

694

695 Plate I - Scanning electron microscope images from ODP Site 1051 that illustrate  
696 morphological development within the clade leading to *Orbulinoides beckmanni*.  
697 Scale bars are 100  $\mu\text{m}$ . (a) *Subbotina senni*, Sample 1051B 7H-5, 65-66 cm. (b)  
698 *Globigerinatheka subconglobata*, Sample 1051B 9H-5, 35-37 cm. (c)  
699 *Globigerinatheka barri*, Sample 1051B 9H-5, 35-37 cm. (d) *Globigerinatheka*  
700 *kugleri*, Sample 1051B 11H-2, 65-67 cm. (e) *Globigerinatheka curryi*, Sample 1051B

701 11H-3, 131-133 cm. (f) *Globigerinatheka mexicana*, Sample 1051B-11H-4, 65-67  
702 cm. (g) *Globigerinatheka euganea*, Sample 1260A 6R-1, 7-8.5 cm. (h)  
703 *Globigerinatheka euganea*, Sample 1051B 11H-3, 145-147 cm. (i) *Orbulinoides*  
704 *beckmanni*, Sample 1051B 11H-3, 131-133 cm. (j) *Orbulinoides beckmanni*, Sample  
705 1051B 9H-5, 35-37 cm. (k) *Orbulinoides beckmanni*, Sample 1051B 11H-3, 131-133  
706 cm. (l) *Orbulinoides beckmanni*, Sample 1051B 9H-5, 5-7 cm.

707

708 Plate II - Scanning electron microscope images from ODP Sites 1051 and 1260 that  
709 illustrate morphological variability within *Orbulinoides beckmanni*. Scale bars are  
710 100  $\mu\text{m}$ . (a) *Orbulinoides beckmanni*, Sample 1051B 8H-2, 105-107 cm. (b)  
711 *Orbulinoides beckmanni*, Sample 1051B 8H-2, 105-107 cm. (c) *Orbulinoides*  
712 *beckmanni*, Sample 1051B 8H-2, 105-107 cm. (d) *Orbulinoides beckmanni*, Sample  
713 1051A 8H-4, 45-47 cm. (e) *Orbulinoides beckmanni*, Sample 1051A 8H-4, 45-47 cm.  
714 (f) *Orbulinoides beckmanni*, Sample 1051A 8H-4, 45-47 cm. (g) *Orbulinoides*  
715 *beckmanni*, Sample 1051A 8H-6, 5-7 cm. (h) *Orbulinoides beckmanni*, Sample  
716 1051A 8H-6, 5-7 cm. (i) *Orbulinoides beckmanni*, Sample 1051A 8H-6, 5-7 cm. (j)  
717 *Orbulinoides beckmanni*, Sample 1260A 6R-1, 7-8.5 cm. (k) *Orbulinoides*  
718 *beckmanni*, 1260A 6R-1, 7-8.5 cm. (l) *Orbulinoides beckmanni*, Sample 1260A 6R-1,  
719 7-8.5 cm.

720

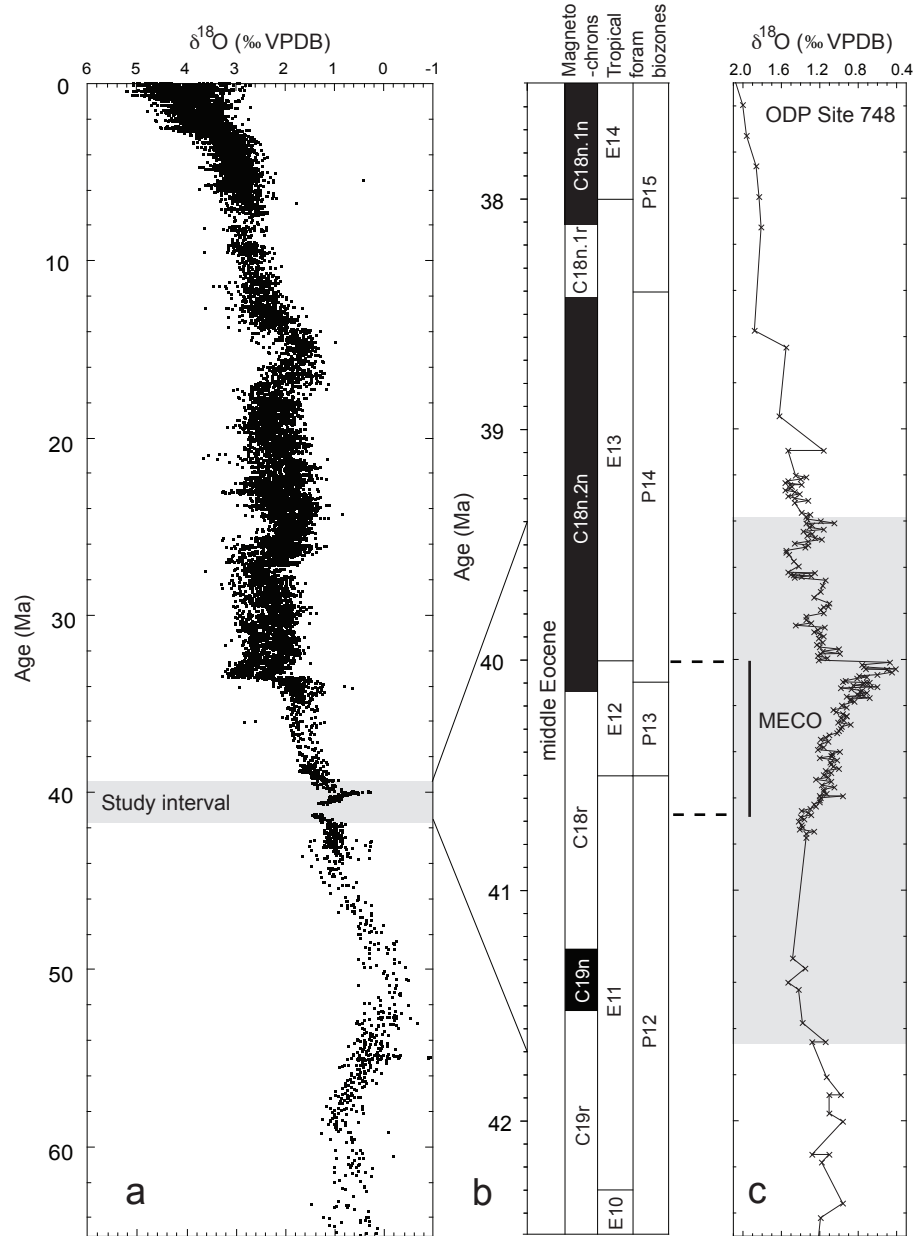
721 **Table 1** – Polarity zones and interpretation of chrons for ODP Site 1051.

722

723 **Table 2** – Comparison of magnetobiochronology of planktonic foraminiferal datum  
724 events identified by Berggren et al. (1995), \*Wade (2004), and this study.

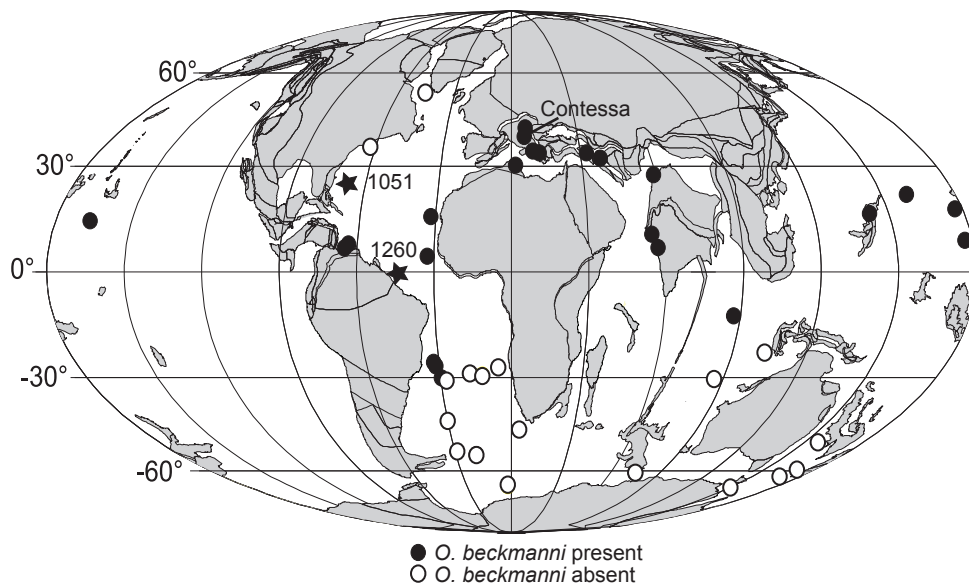
725

726  
727



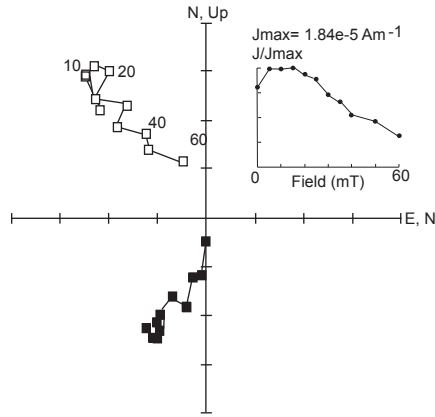
Edgar\_Figure 1



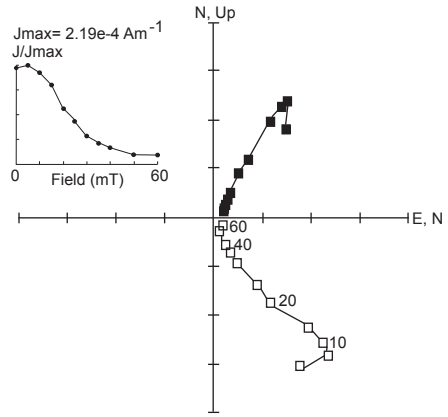


Edgar\_Figure 2

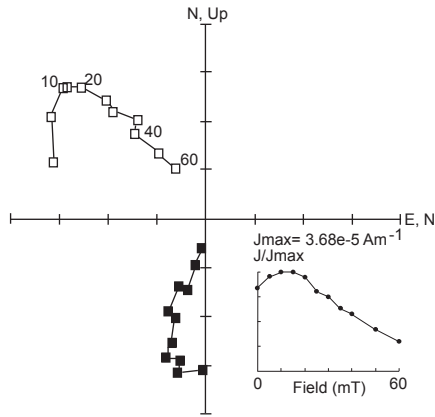
**A** 1051B 15H-6, 94 cm



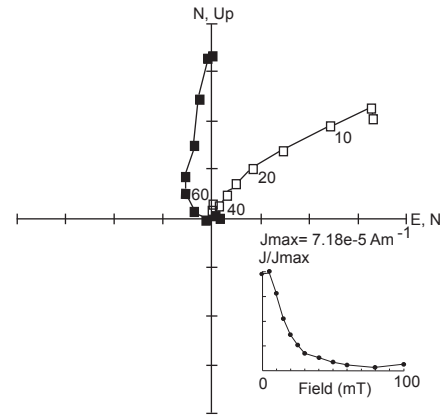
**B** 1051B 15H-2, 22 cm



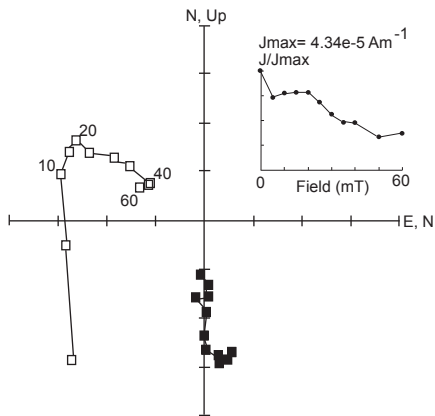
**C** 1051B 14H-7, 29 cm



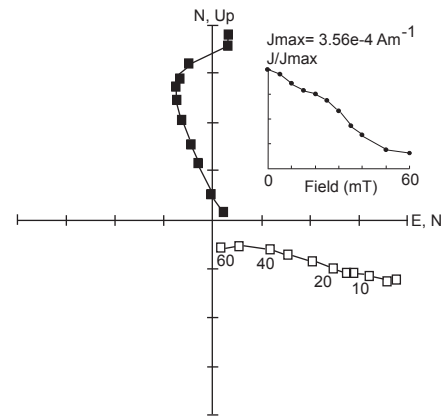
**D** 1051B 12H-2, 48 cm



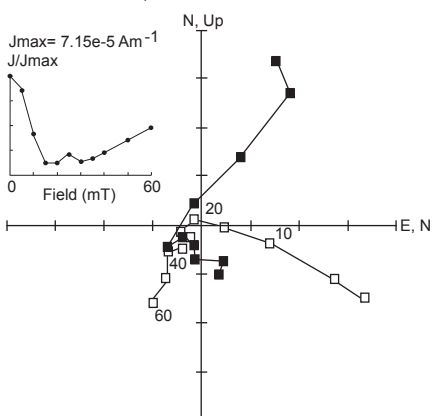
**E** 1051B 11H-1, 48 cm



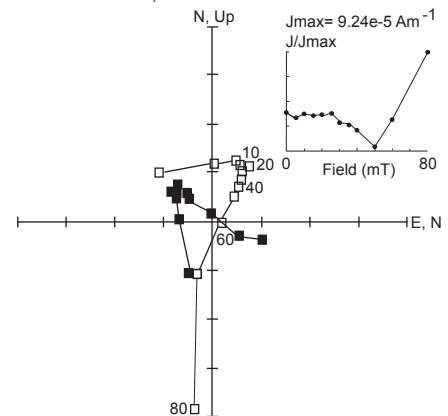
**F** 1051B 9H-2, 35 cm

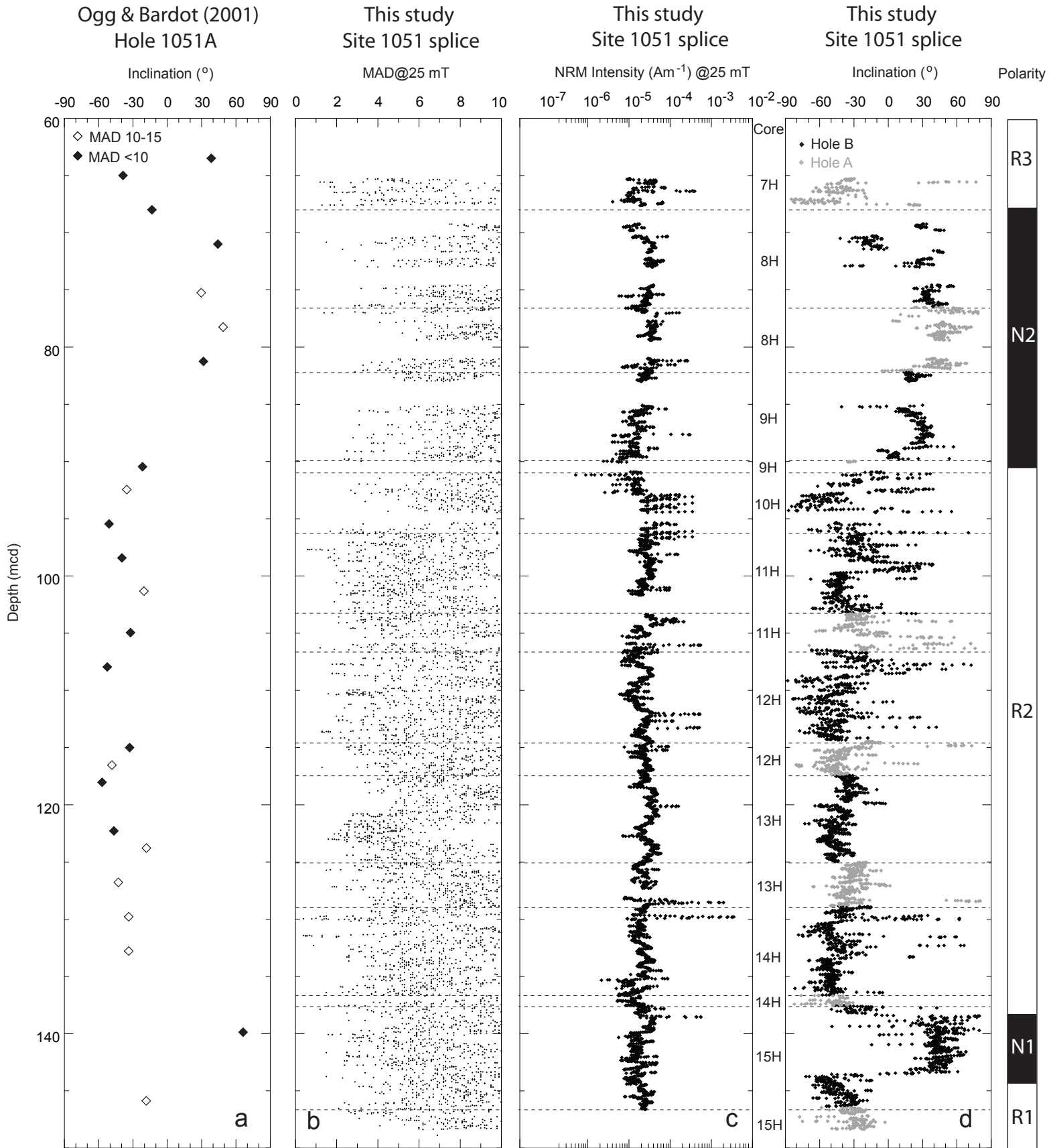


**G** 1051B 9H-6, 138 cm

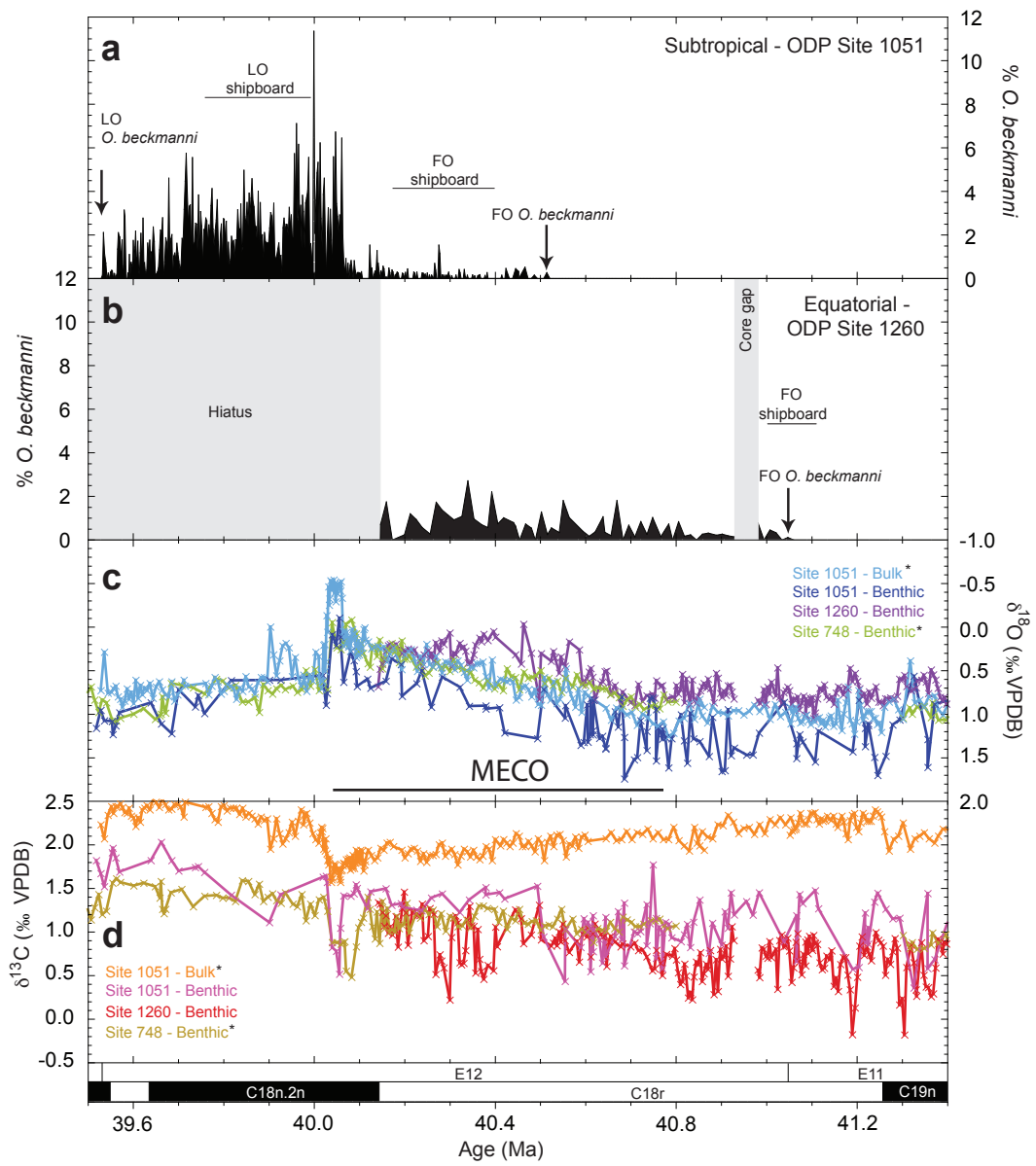


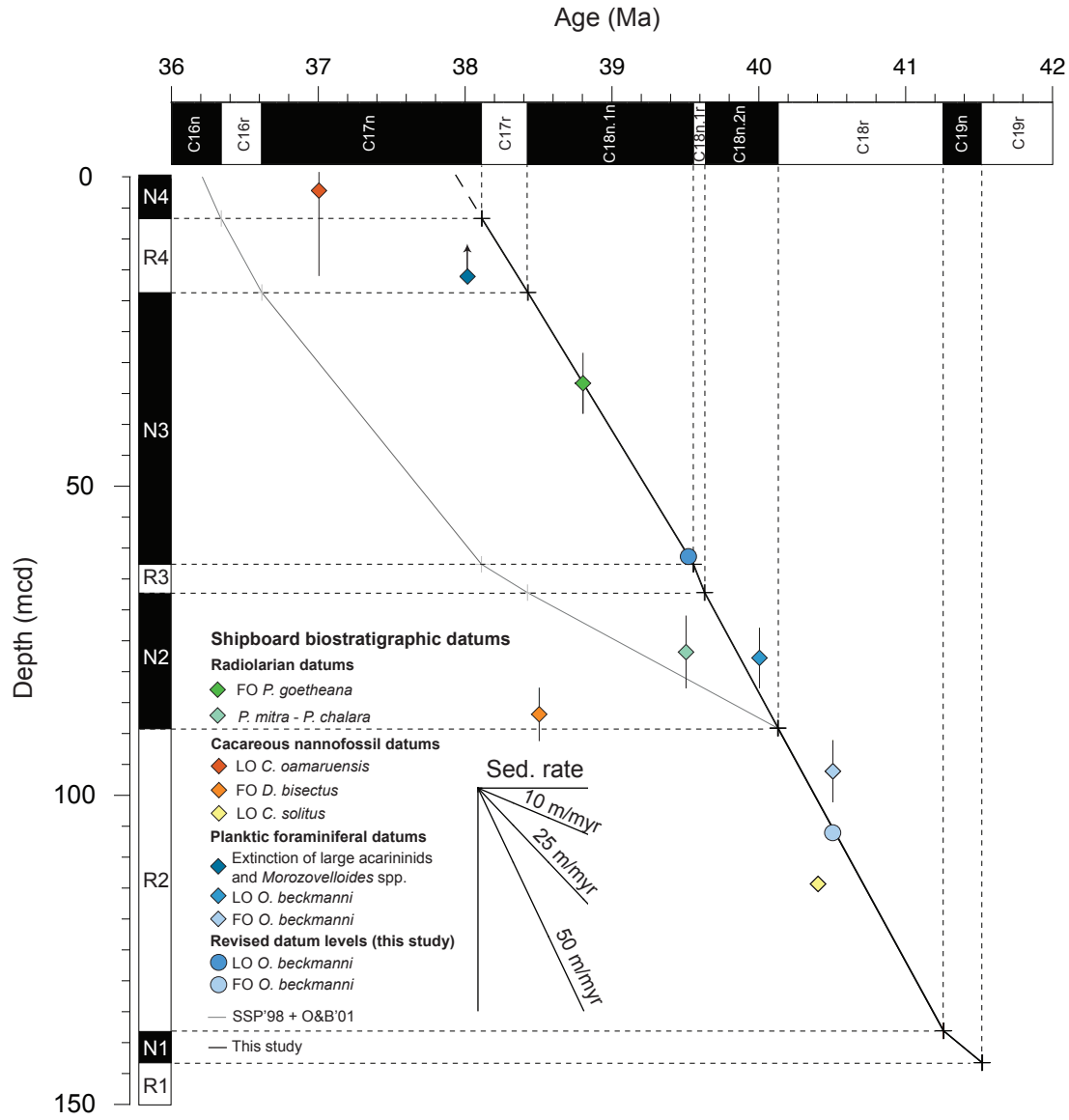
**H** 1051A 7H-3, 15 cm

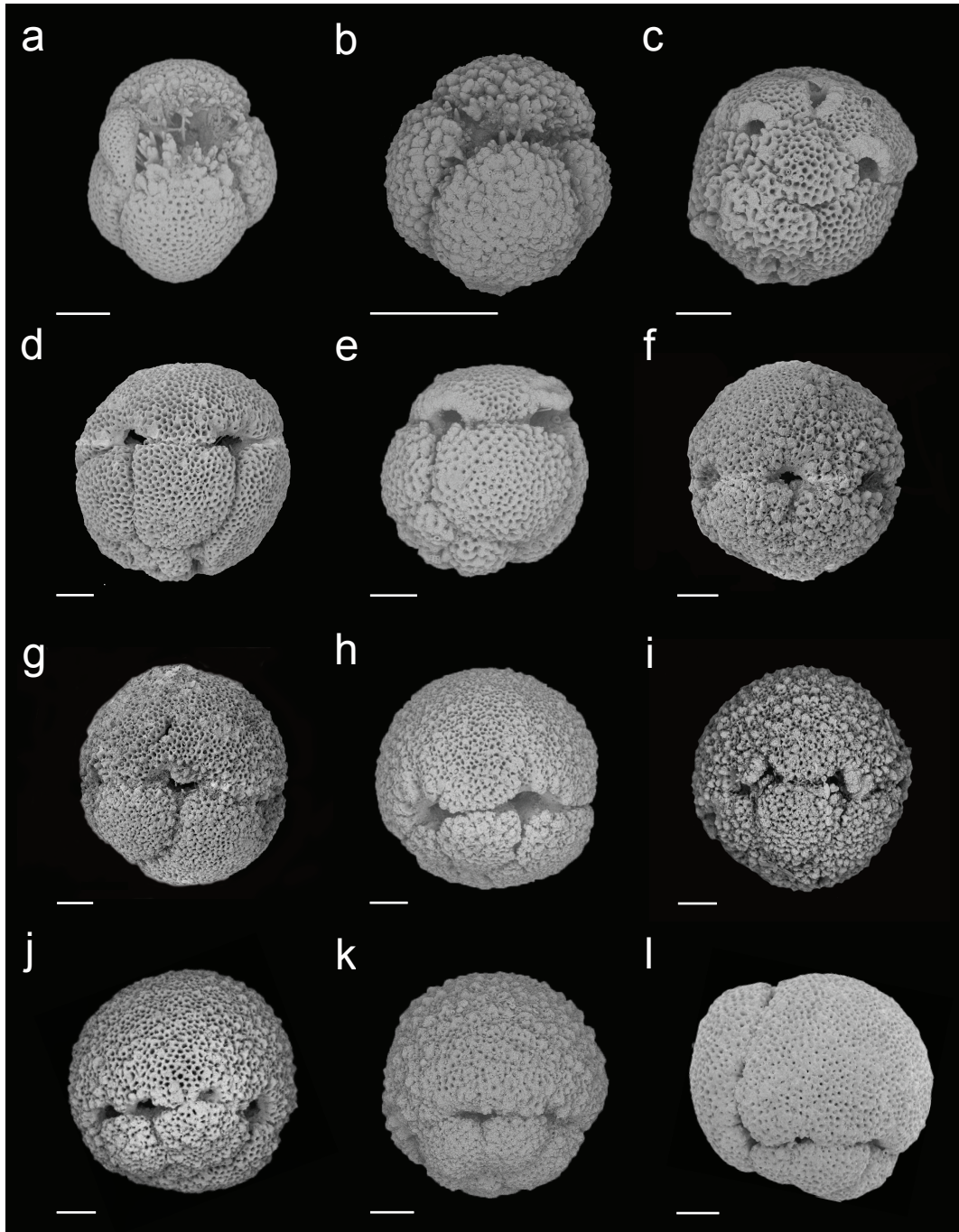




Edgar\_Figure 4







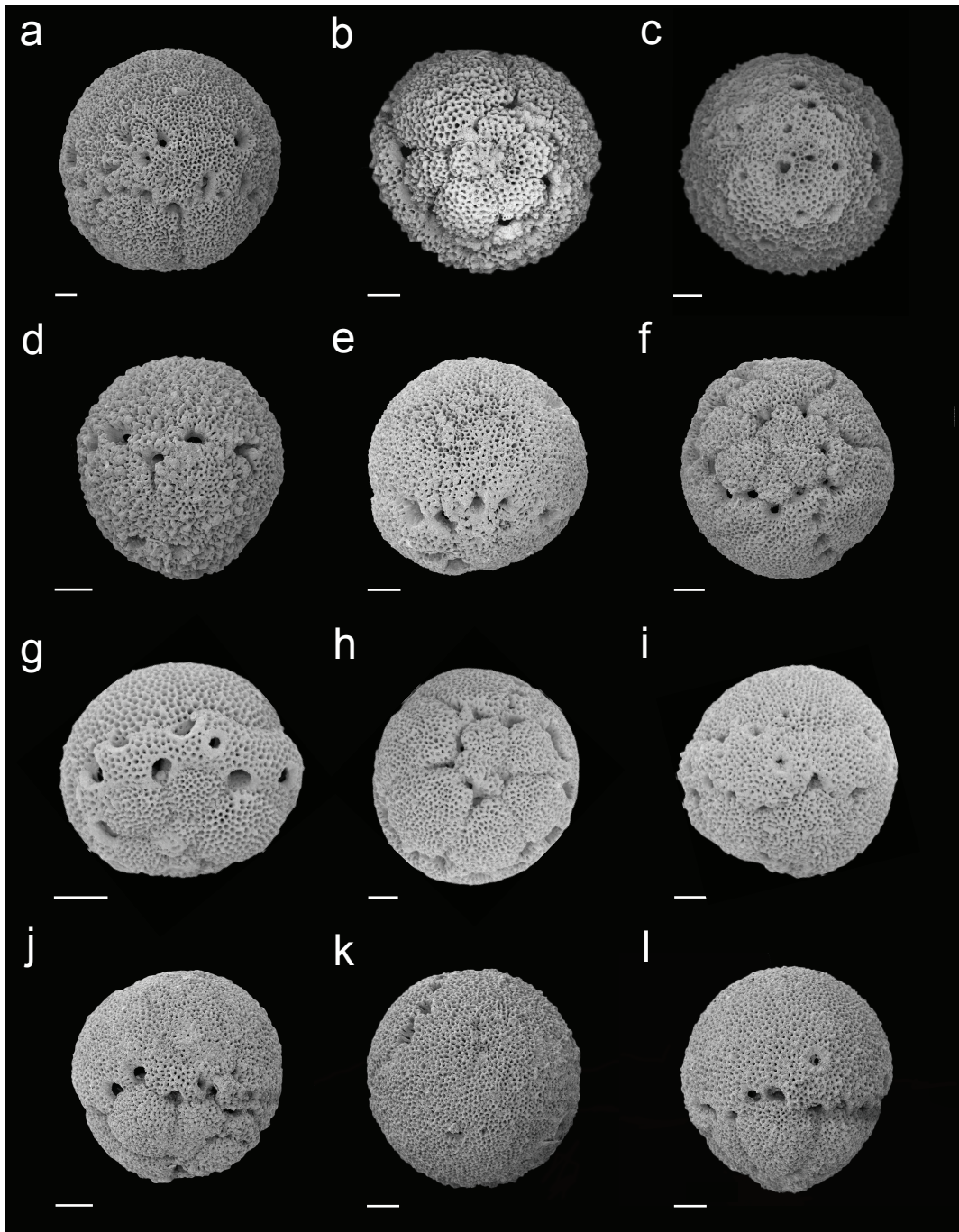


Table 1

Polarity zone	Chron (base)	OB&'01		This study		Age CK95 (Ma)
		T (mcd)	B (mcd)	T (mcd)	B (mcd)	
-	C16n	7.00*	-	-	-	36.410
-	C16r	19.00*	-	-	-	36.618
N4	C17n	60.35	65.00	7.00*	-	38.113
R4	C17r	68.00	71.00	19.00*	-	38.426
N3	C18n.1n	-	-	60.35	65.00	39.552
R3	C18n.1r	-	-	67.52	67.54	39.631
N2	C18n.2n	-	-	88.90	90.00	40.130
R2	C18r	135.78	139.88	138.41	138.43	41.257
N1	C19n	142.88	145.88	143.52	143.54	41.521

Magnetochron ages from Cande and Kent (1992, 1995) referred to as CK95. N = normal, R = reverse, T = top, B = base and mcd = meters composite depth. \* = magnetochron boundaries from the Shipboard Scientific Party (1998). OB&'01 data from Ogg and Bardot (2001).



Datum	Shipboard study		Age CK95 (Ma)	Age GPTS04 (Ma)	This study		New Age CK95 (Ma)	Age GPTS04 (Ma)
	T (mcd)	B (mcd)			T (mcd)	B (mcd)		
<b>ODP Site 1051</b>								
HO <i>O. beckmanni</i>	73.26	82.95	40.0*	39.4	61.80	61.90	39.5	39.0
LO <i>O. beckmanni</i>	91.45	101.35	40.5	39.8	106.15	106.45	40.5	39.8
<b>ODP Site 1260</b>								
LO <i>O. beckmanni</i>	57.80	59.30	40.5	39.8	58.87	59.17	41.0	40.4

Geomagnetic polarity time scales of Cande and Kent (1992, 1995) = CK95 and Gradstein et al., 2004 = GPTS04. LO and HO are lowest and highest occurrences, T = top and B = base, mcd = metres composite depth and \* = Wade (2004).